ISSN 1648-4142 / eISSN 1648-3480

Article in press

VILNIUS TECH Vilnius Gediminas Technical University

TRANSPORT

https://doi.org/10.3846/transport.2026.22870

Special Issue on INTELLIGENT TRANSPORT SYSTEMS AND SMART LOGISTICS

Original Article

MULTI-OBJECTIVE ELECTRIC VEHICLE COLD CHAIN LOGISTICS LOCATION-ROUTING PROBLEM WITH CHARGING-STATIONS

Yi LIU ✉

School of Logistics, Beijing Wuzi University, Beijing, China

Highlights:
- proposes the ECC-LRP-CS integrating depot location, EV routing, and charging-station placement;
- develops a multi-objective model minimizing logistics cost while maximizing network efficiency;
- proposes an integrated IAFSA and LCOA algorithm to solve the NP-hard problem effectively;
- provides sensitivity analysis of battery range and speed to support cold chain logistics decisions;
- addresses carbon neutrality goals by electrifying cold chain logistics networks.

Article History:
- submitted 20 July 2022;
- resubmitted 31 March 2023;
- accepted 29 April 2023;
- first published online 31 July 2026.

Abstract. This study focuses on an Electric Vehicle (EV) cold chain logistics location-routing problem with charging-stations that aims at optimizing the location of depots, the delivery routing of EVs, the time planning for visiting all customers and the location of charging-stations. To tackle this problem, a multi-objective optimization model is established to minimize cold chain logistics cost, and at the same time maximize cold chain logistics network efficiency. An integrated algorithm that combines an Improved Artificial Fish Swarm Algorithm (IAFSA) and a Label-based Charging-station Optimization Algorithm (LCOA) is used to solve the proposed model. Extensive computational experiments are conducted to demonstrate the applicability of the proposed model, and show the efficiency of the developed algorithm. Moreover, the effects of battery driving range and traveling speed on the results are explored through the sensitivity analysis that provides decision supports for logistics enterprises to operate an EV cold chain logistics network.

Keywords: cold chain logistics, electric vehicle, location-routing problem, charging-station, multi-objective optimization, artificial fish swarm algorithm.

✉ E-mail: *16114209@bjtu.edu.cn*

Notations

Abbreviations:

AFSA – artificial fish swarm algorithm;
APF – approximate Pareto front;
CV – combustion vehicle;
ECC-LRP-CS – EV cold chain logistics location-routing problem with charging-stations;
ELRP – EV location-routing problem;
EV – electric vehicle;
EVRP – EV routing problem;
IAFSA – improved AFSA;
LCOA – label-based charging-station optimization algorithm;
NA – numerical algorithm;
RPF – real Pareto front.

Sets:

C – set of customers;
D – set of candidate depots;
K – set of EVs;
S – set of candidate charging-stations;
V – set of all nodes, i.e., $V = D \cup S \cup C$.

Variables:

$b_{\min}$ – minimal remaining battery power [kW·h];
C^{ev} – loading capacity of the EVs [kg];
C_B – battery capacity [kW·h];
C^{ev}_{ik} – cargo demand of EV k at node i [kg];
C^D_j – capacity of depot j [kg];
c_e – electricity price [¥/kW·h];
c^d_i – construction cost for depot i [¥];
c^f_k – fixed use cost for EV k [¥];

c_k^r – renting cost of EV k [¥/h];
c_k^s – driver salary [¥/h];
c_l – late cost per time [¥/h];
c_s^o – fixed cost of opening charging-station s [¥];
c_w – waiting per time [¥/h];
c_1 – refrigeration cost in the transportation process [¥/h];
c_2 – refrigeration cost in the unloading process [¥/h];
d_i^c – customer demand [kg];
E_{ik}^a – battery power once EV k arrives charging-station i [kW·h];
E_{ik}^{ava} – usable battery power when EV k leaves node i [kW·h];
E_{ik}^d – battery power once EV k leaves charging-station i [kW·h];
e_i – earliest allowed service time of customer i;
l_i – latest allowed service time of customer i;
N_{MV} – maximum amount of the EVs at the depot;
P_{ik} – time penalty cost when EV k arrives at customer i [¥/kg];
p – unit price of goods [¥/kg];
p_v^c – speed-related unit distance power consumption [kW·h/km];
T_j^D – hard time window of depot j;
t_i^s – service time, i.e., unloading time of the EV for customer i [h];
t_{ijk} – traveling time between i and j of EV k [h];
t_{ik}^a – time once EV k arrives at customer i;
t_{ik}^d – arrival time delay [h];
t_{ik}^w – waiting time [h];
t_{sk}^c – charging time [h];
u_b – utilization efficiency of the battery capacity [%];
v – traveling speed of the EVs [km/h];
α – rate of deterioration in the transportation process;
β – rate of deterioration in the unloading process;
Φ_i – visited customers set of EV k when it begins to serve customer i;
Ψ – sufficiently large positive number.

Decision variables:

x_{ijk} – 1 if arc (i, j) is travelled by EV k and 0 otherwise;
y_j – 1 if candidate depot j is constructed and 0 otherwise;
z_s – 1 if candidate charging-station s is constructed and 0 otherwise.

1. Introduction

The achievement of carbon neutrality target has been a task of top priority in developing low-carbon economy. As the low temperature environment should be maintained to make sure the quality of the frozen product, the cold chain logistics has the characteristic of high carbon emission in the logistics industry. James, S. J. & James, C. (2010) illustrate that the amount of carbon emission from cold chain logistics accounted for nearly 1% of the global carbon emission. Meanwhile, with the rapid growth of demands for seafood, fruit, vaccines and other temperature-sensitive products, the cold chain logistics is advancing rapidly. To achieve the goals of carbon peak and carbon neutralization, it is necessary to build a low-carbon cold chain logistics system to deal with the prominent contradiction between the carbon emission control and the scale expansion of cold chain logistics. Therefore, the low-carbon cold chain logistics has been a research highlight. For example, Wang *et al.* (2017), Zhang *et al.* (2019c), Leng *et al.* (2020) and Song *et al.* (2020) consider the carbon emission cost of CVs in the cold chain logistics routing optimization model.

EVs are considered as an effective way of reducing carbon emissions that makes them strongly popularized by the governments around the world (Zhang *et al.* 2019b). Therefore, it is becoming increasingly important to establish a sustainable cold chain logistics network with the usage of EVs instead of CVs. Nevertheless, EVs are still facing weaknesses related to range anxiety (Sassi, Oulamara 2017), long recharging time (Jung, Jayakrishnan 2012) and lack of availability of charging infrastructures (Eggers, Fe., Eggers, Fa. 2011). Therefore, to realize the electrification of cold chain logistics network, an ECC-LRP-CS is firstly proposed in this study, which considers as an integrated optimization of the location of depots, the delivery routing of EVs, the time planning for visiting all customers and the location of charging-stations.

Currently, some related studies have discussed the EVRP (e.g., Zhang *et al.* 2020; Bac, Erdem 2021), while not considering the charging infrastructures location problem. It is a key decision to select the optimal location of the charging infrastructure to minimize the construction cost and distribution cost. The ELRP is relatively recent even if it can achieve environmental benefits (Çalık *et al.* 2021). Yang & Sun (2015), Hof *et al.* (2017), Jie *et al.* (2019), Zhang *et al.* (2019b) and Sayarshad *et al.* (2020) research the ELRP with battery swap station. Although battery swap takes less time to replace the battery, additional land needs to be purchased or leased to build a battery warehouse for storing the battery pack. Recharging by charging-station is the most common way for EVs, which can divided into full recharging (Ghobadi *et al.* 2021) and partial recharging (Schiffer, Walther 2017). Nevertheless, the abovementioned studies focus on ordinary logistics, while not taking into account cold chain logistics. Also, the location of depots is not considered. Zhao *et al.* (2020) consider the use of EVs in cold chain logistic distribution, while not taking into account the charging infrastructure and depot location problems.

The introduction of EVs will add the complexity of the associated cold chain logistics LRP including modelling and algorithm designing. Common ground in literature is the lack of an effective approach to design the ECC-LRP-CS. Therefore, this study aims at integrating EVs into the cold chain logistics to firstly optimize ECC-LRP-CS to achieve sustainable development targets including reducing carbon emission and logistics cost, and improving customer satisfaction. A multi-objective optimization model is presented to address the simultaneous optimization problem of the location of depots, the delivery routing of EVs, the time planning for visiting all customers and the location of charging-stations. The 1st objective is the minimization of cold chain logistics cost, whereas the 2nd objective aims at maximizing cold chain logistics network efficiency.

Given that LRP is NP-hard, many heuristics have been proposed for solving this problem and its variations (Lin, Kwok 2006). For instance, population metaheuristics (Koç *et al.* 2016; Zhang *et al.* 2019c), simulated annealing (Yu *et al.* 2021) and adaptive large neighbourhood search algorithms (Yang, Sun 2015), in which the AFSA is the typical population metaheuristic that mimics the foraging activities of fish swarm (Li 2002). With the characteristic of parallel executing swarming, following, preying and random behaviours, the AFSA has the strong search ability and the fast convergence speed to find the global optimal solution and does not ask for much on the initial solutions, and has been widely used to solve travelling salesman problem (Yang 2014), multidimensional knapsack problem (Azad *et al.* 2014), reliability-redundancy application problem (He *et al.* 2015), multi-objective fuzzy disassembly line balancing problem (Zhang *et al.* 2017), cold chain logistics VRP (Song *et al.* 2020) and so on. Moreover, the IAFSA is considered as an efficient algorithm for multi-objective problems, achieving a set of Pareto-efficient solutions (Zhang *et al.* 2017; Liu *et al.* 2020b). As far as we know, the AFSA has not yet been developed for cold chain logistics LRP. Therefore, an integrated algorithm that combines an IAFSA and a LCOA is used to tackle the presented model in this study. The IAFSA can take input from external procedure-based declarations (i.e., LCOA) during the optimization process. Moreover, in AFSA-based optimization, one can, in order to improve efficiency, incorporate problem-specific information and expertise during the optimization process (by appropriately modifying the fish-swarm behaviours) or at its start (by appropriately determining the initial fish swarm). Furthermore, the proposed algorithm handles boundary conditions on decision variables through coding of variables. It ensures that variables are always within the stated bounds. As a result, the above characteristics of the proposed algorithm make it possible to solve the ECC-LRP-CS to obtain the optimal or near-optimal solutions. In addition, this study compares with the designed instances that solved by the NA to assess the quality of obtained results, and also adopts performance metrics to assess the performance of the developed algorithm in the ECC-LRP-CS. Furthermore, the sensitivity analyses of battery driving range and the traveling speed of EVs are proposed.

Therefore, the principal contributions of this study are as follows:

- our work is the 1st to study the ECC-LRP-CS by jointly optimizing the location of depots, the delivery routing of EVs, the time planning for visiting all customers and the location of charging-stations, while several practical constraints, like soft time windows, capacity limitation of depot, energy consumption of EVs, are considered;
- a multi-objective optimization model is defined for the ECC-LRP-CS in which environmental, logistics enterprise, and customers are all considered;
- an integrated algorithm framework is developed, where the IAFSA is used to tackle the LRP with time windows, and the LCOA is developed to deal with the charging-station location problem in the cold chain logistics network.

The remainder of this article is organized as follows: Section 1 – is introduction, in Section 2 the multi-objective optimization model is proposed; Section 3 provides the solution method for the ECC-LRP-CS. Section 4 gives the computational experiments and reports analyses of the results, followed by Section 5 (conclusions).

2. Model establishment

2.1. Problem description

The ECC-LRP-CS is defined on a complete and directed graph, which combines a customer set, a candidate depot set, a candidate charging-station set and an edge set, as shown in Figure 1. Each customer has a delivery demand, a service time and a soft time window. Each candidate depot has a capacity and a time window. Only EVs are considered, and each of them executes at most one trip. Each customer is served only once by an EV and depot. One cargo type is considered. The total cargo of each EV cannot exceed its loading capacity. At the beginning of the distribution work, each EV leaves the depot to service the customers, then returns back before closing time. During the service, if the EVs need to be recharged, any charging-station can be selected. Moreover, each EV starts charging as soon as it reaches the charging-station, and does not consume electricity when servicing customers. Furthermore, the real traffic conditions are not considered, i.e., the traveling speed of the vehicles is constant. The change of ambient temperature outside the carriage only affects the consumption of refrigeration equipment. The temperature in the refrigerated carriage is constant during transportation. The demand, location and soft time window of each customer, and the locations of each candidate depot and each candidate charging-station are deterministic and known in advance.

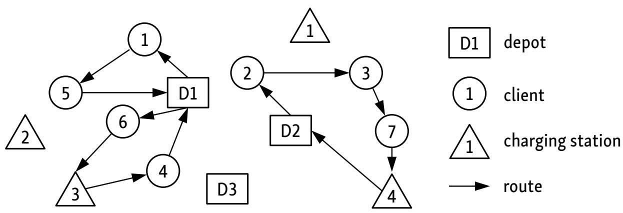

Figure 1. Example ECC-LRP-CS route chart

2.2. Model

A multi-objective optimization model of the ECC-LRP-CS is proposed. The objectives are to minimize cold chain logistics cost and maximize cold chain logistics network efficiency. The 1st objective Z_1 addresses 6 components, i.e., fixed cost C_1 including the construction cost for depots and the fixed use cost for EVs, variable cost C_2 dependent on the total traveling time containing the renting cost of EVs and the driver salary, power consumption cost during the distribution process C_3, refrigeration cost C_4 including those during transportation and the process of unloading, recharging cost C_5, and construction cost for charging-stations C_6, as shown in Equations (3)–(8). The 2nd objective Z_2 is realized by minimizing the total penalty cost, including time penalty cost C_7 aiming at completing the distribution of cold chain products within the specified time period in Equations (9) and (10) and cargo damage cost C_8 including the damage cost for the transportation process and the open-door process in Equation (11) (Leng *et al.* 2020).

$$\min Z_1 = \min\left(C_1 + C_2 + C_3 + C_4 + C_5 + C_6\right); \tag{1}$$

$$\min Z_2 = \min\left(C_7 + C_8\right); \tag{2}$$

$$C_1 = \sum_{i \in D} c_i^d \cdot y_i + \sum_{k \in K} \sum_{i \in D} \sum_{j \in C} c_k^f \cdot x_{ijk}; \tag{3}$$

$$C_2 = \sum_{k \in K} \sum_{i \in D} \sum_{j \in C} t_{ijk} \cdot x_{ijk} \cdot \left(c_k^r + c_k^s\right); \tag{4}$$

$$C_3 = c_e \cdot p_v^c \cdot v \cdot \sum_{k \in K} \sum_{i, j \in V, i \neq j} t_{ijk} \cdot x_{ijk}; \tag{5}$$

$$C_4 = c_1 \cdot \sum_{k \in K} \sum_{i, j \in V, i \neq j} x_{ijk} \cdot t_{ijk} + c_2 \cdot \sum_{i \in C} t_i^s; \tag{6}$$

$$C_5 = c_e \cdot \sum_{k \in K} \sum_{i \in S} \sum_{j \in C \cup D} \left(E_{ik}^d - E_{ik}^a\right) \cdot x_{ijk}; \tag{7}$$

$$C_6 = \sum_{s \in S} c_s^o \cdot z_s; \tag{8}$$

$$C_7 = \sum_{k \in K} \sum_{i \in C} P_{ik}; \tag{9}$$

$$P_{ik} = \begin{cases} c_w \cdot \left(e_i - t_{ik}^a\right), & t_{ik}^a < e_i; \\ 0, & e_i \le t_{ik}^a \le l_i; \\ c_l \cdot \left(t_{ik}^a - l_i\right), & t_{ik}^a > l_i; \end{cases} \tag{10}$$

$$C_8 = p \cdot \sum_{k \in K} \sum_{i \in C} \sum_{j \in V} \left(d_i^c \cdot x_{ijk} \cdot \left(1 - e^{-\alpha \cdot \left(\max\left(t_{ik}^a, e_i\right) - \sum_{j \in \Phi_i} t_j^s \right)} \right) \right) + p \cdot \sum_{k \in K} \sum_{i \in C} \sum_{j \in V} \left(d_i^c \cdot x_{ijk} \cdot \left(1 - e^{-\beta \cdot \sum_{j \in \Phi_i} t_j^s} \right) \right). \tag{11}$$

Constraint (12) indicates that each customer should be served only once. Constraint (13) is the flow conservation. Constraint (14) ensures that each customer is only served by one EV. The capacity limitation of EVs is established by Constraint (15). Constraint (16) guarantees that the EV capacities are always respected.

$$\sum_{k \in K} \sum_{i \in V} x_{ijk} = 1, \ \forall j \in C; \tag{12}$$

$$\sum_{k \in K} \sum_{i \in V} x_{ijk} = \sum_{k \in K} \sum_{i \in V} x_{jik}, \ \forall j \in C; \tag{13}$$

$$x_{ijk} + \sum_{g \in K, k \neq g} \sum_{m \in V} x_{jmg} \le 1, \ \forall i \in V, \ j \in C, \ k \in K; \tag{14}$$

$$0 \le C_{ik}^{ev} \le C^{ev}, \ \forall i \in D, \ k \in K; \tag{15}$$

$$0 \le C_{jk}^{ev} \le C_{ik}^{ev} - d_i^c \cdot x_{ijk} + C^{ev} \cdot \left(1 - x_{ijk}\right), \ \forall i, \ j \in V, \ i \neq j, \ k \in K. \tag{16}$$

Constraints (17)–(22) are time window constraints. Constraints (17) and (18) guarantee that each EV is able to service in its own time window. Constraints (19) and (20) calculate the waiting time if the EV reaches earlier and the punishment for time delay, respectively. The constraint on the time windows for depots is shown in Constraint (21). Constraint (22) indicates the time relationship between customers.

$$t_{ik}^a \le l_i, \ \forall k \in K; \tag{17}$$

$$e_i \le \left(t_{ik}^a + t_{ik}^w\right) \le l_i, \ \forall k \in K; \tag{18}$$

$$t_{ik}^w = \max\left(0, e_i - t_{ik}^a\right), \ \forall k \in K; \tag{19}$$

$$t_{ik}^d = \max\left(0, t_{ik}^a - l_i\right), \ \forall k \in K; \tag{20}$$

$$t_{jk}^a \le T_j^D, \ \forall j \in D, k \in K; \tag{21}$$

$$t_{jk}^a \ge t_{ik}^a + t_{ik}^w + t_i^s + t_{ijk} - t_{ik}^d + \left(1 - x_{ijk}\right) \cdot \Psi, \ i \in C, j \in V, i \neq j, k \in K. \tag{22}$$

Constraints (23)–(29) are depot constraints. Constraints (23) and (24) enforce the routes should start and end at a same depot. Constraint (25) limits the depot capacity. Constraint (26) guarantees that each customer must be served by only one depot. Constraints (27) and (28) state the logical relationship between the open of the depot and the service activities. Constraint (29) restricts the amount of total EVs at the depot.

$$\sum_{i \in C \cup S} x_{ijk} = \sum_{i \in C} x_{jik}, \ \forall k \in K, j \in D; \tag{23}$$

$$x_{ijk} + x_{imk} + \sum_{n \in D, m \neq n} x_{jnk} \le 2, \ \forall k \in K, i, j \in C, m \in D; \tag{24}$$

$$\sum_{k \in K} \sum_{i \in C} d_i^c \cdot x_{ijk} \le C_j^D \cdot y_j, \ \forall j \in D; \tag{25}$$

$$\sum_{j \in D} x_{ijk} = 1, \ \forall k \in K, i \in C; \tag{26}$$

$$x_{ijk} \le y_j, \ \forall k \in K, i \in C, j \in D; \tag{27}$$

$$\sum_{k \in K} \sum_{i \in C} x_{ijk} \ge y_j, \ \forall j \in D; \tag{28}$$

$$\sum_{k \in K} \sum_{i \in V} x_{ijk} = \sum_{k \in K} \sum_{i \in V} x_{jik} \le N_{MV}, \ \forall j \in D. \tag{29}$$

Constraints (30)–(32) are charging-station constraints. Constraints (30) and (31) state the logical relationship between the construction of the charging-station and the recharging activities. Constraint (32) states that the arrival time at node j by EV k cannot be earlier than the time when it leaves the charging-station s plus the traveling time during the distribution.

$$E_{sk}^{d} \le C_B \cdot z_s,\ \forall s \in S,\ k \in K; \tag{30}$$

$$z_s \le E_{sk}^{d},\ \forall s \in S; \tag{31}$$

$$t_{jk}^{a} \ge \left(t_{sk}^{a} + t_{sjk} + t_{sk}^{c}\right) \cdot x_{sjk},\ s \in S,\ j \in V,\ s \ne j,\ k \in K. \tag{32}$$

Constraints (33)–(37) are energy consumption constraints. Constraint (33) guarantees that each EV has adequate remaining battery power to visit the charging-station and the depot. Constraint (34) indicates that the battery power of EV k at node j cannot larger the usable battery power when EV k leaves node i subtracts the battery power consumed between nodes i and j. Constraint (35) ensures that each EV is fully recharged from the depot. Constraint (36) ensures that the battery is not overcharged.

$$E_{ik}^{ava} = u_b \cdot E_{ik}^{d} - b_{\min},\ \forall i \in D \cup S; \tag{33}$$

$$E_{jk}^{a} \le E_{ik}^{ava} - v \cdot p_v^c \cdot t_{ijk} \cdot x_{ijk} + C_B \cdot \left(1 - x_{ijk}\right),\ \forall i, j \in V,\ i \ne j,\ k \in K; \tag{34}$$

$$E_{ik}^{d} = C_B,\ \forall i \in D,\ k \in K; \tag{35}$$

$$0 \le E_{sk}^{d} \le C_B,\ \forall s \in S,\ k \in K. \tag{36}$$

3. Solution method for the ECC-LRP-CS

This section develops an integrated algorithm in which the IAFSA is embedded with a LCOA to solve the ECC-LRP-CS. The general framework of the integrated algorithm is given in Algorithm 1. Generate the initial population according to the initialization procedure (line 1). Then an artificial fish is randomly selected from the population to sequentially execute preying, swarming and following behaviours, while the random behaviours are executed as supplementary, to optimize the location of depots, the delivery routing of EVs and the time planning for visiting all the customers (lines 3…6). Subsequently, the LCOA is presented to tackle the charging-station location problem for each delivery route (line 7). The modified food concentration applied to evaluate the solution is determined by the ranking and density values, which calculate based on the objectives (line 8) (Liu *et al.* 2020b). After that, update the elitist set (line 9) and generate the next generation according to it (line 10). Specifically, if the amount of elitist solutions in the elitist set is less than N_{Pop}, the solutions from current population on the basis of their food concentrations from large to small together with the elitist set are formed the population in the next generation. Otherwise, the N_{Pop} solutions from the elitist set are selected based on the density values from small to large to form the population in the next generation. When $\max_{gen}$ is reached, the proposed algorithm terminates (line 11). The concrete implementation of the developed algorithm is given in the follows.

3.1. Initialization

Figure 2 describes a solution (i.e., an artificial fish) encoding. A 2-step initialization procedure is used to generate an initial artificial fish, then copy an initial artificial fish to N_{Pop} to construct the initial population:

- *Step 1*: Assign customers to depots. Determine the closest depot for each customer, then assign each customer to its nearest depot without violating the depot capacity. Due to depot capacity constraint, if the customers cannot be assigned to their nearest depots, they will be assigned to their sub-nearest depot, and so on until all customers are assigned. Create a list $List_d$ to store the customers corresponding to the depot d;
- *Step 2*: Construct routes for each depot;
- *Step 2.1*: Select a depot d;
- *Step 2.2*: Assume that each customer is served by a unique EV. Construct $|List_d|$ routes and put them into list $List_r$;
- *Step 2.3*: If the route in the $List_r$ satisfies the range constraint, it will put into list $List_f$, otherwise put into list $List_{nonf}$;
- *Step 2.4*: Select a route r in $List_{nonf}$, then insert a charging-station s from the candidate charging-station set into a location that minimizes the insertion cost $IC(i, s) = \left(t_{isk} + t_{sdk} - t_{idk}\right) \cdot v$ between node i and depot d. The route r will put into $List_f$ and delete from $List_{nonf}$ if the range constraint is meet after inserting, and delete from $List_{nonf}$ otherwise. The route including multiple charging-stations is not considered at this stage. Repeat Step 2.4 until $List_{nonf}$ is empty;
- *Step 2.5*: By using Insertion Heuristics proposed by Solomon (1987), routes in $List_f$ are merged. 1st, a seed customer i^*, which has the farthest geographical distance compared to the depot or the earliest allowed service time is chosen and deleted from $List_d$. Then a customer c not on the route is selected from $List_d$ to insert into the best feasible insertion place u with a minimum measure, as shown in Equations (37)–(40);
- *Step 2.6*: If the EV capacity constraint is violated, execute Step 2.5 and find a new seed customer from $List_d$. Otherwise, delete customer c from $List_d$, and check whether the newly constructed route meets the range constraint. If the range constraint is not meet, insert a charging-station and execute Step 2.5 until $List_d$ is empty.

$$IC(i, u, j) = \alpha_1 \cdot C_{11}(i, u, j) + \alpha_2 \cdot C_{12}(i, u, j) + \alpha_3 \cdot C_{13}(i, u, j); \tag{37}$$

$$C_{11}(i, u, j) = t_{iuk} + t_{ujk} - \gamma t_{ijk},\ \gamma \ge 0; \tag{38}$$

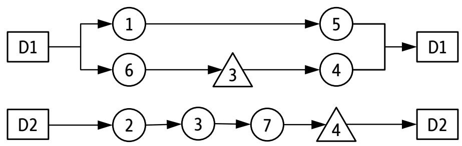

Figure 2. Example of a solution encoding

Algorithm 1. The general framework of the integrated algorithm

1: *Initialization*: initialize a population with size N_{Pop}
2: **while** number of iterations < $\max_{gen}$ do
3: *Selection*: retain the optimal solution and randomly select an artificial fish from the remaining solutions
4: *Fish swarm behaviours*: optimize the location of depots, the delivery routing of EVs and the time planning for visiting all the customers
5: Sequentially execute preying, swarming and following behaviours
6: Execute random behaviours as supplementary according to their historical performance
7: *LCOA*: Optimize the location of charging-stations
8: *Solution evaluating*: Calculate the ranking value and the density value to modify the food concentration
9: *Elitist updating*: Introduce new Pareto optimal solutions and remove dominated ones
10: *Generation updating*: Generate the next generation according to elitist set
11: **end while**
12: Return elitist set

$$C_{12}(i,u,j) = t_{jk}^{a,new} - t_{jk}^{a}; \quad (39)$$

$$C_{13}(i,u,j) = l_u - t_{uk}^{a}, \quad (40)$$

where: α_1, α_2, α_3 are nonnegative weight value, $\alpha_1 + \alpha_2 + \alpha_3 = 1$; $t_{jk}^{a,new}$ is the new arrival time at node j by EV k.

3.2. Fish swarm behaviours

Randomly choose an artificial fish AFS_a from the swarm to sequentially execute preying, swarming and following behaviours, while the random are executed as supplementary, to optimize the locations of depots, the delivery routes and the time planning for visiting all customers. If the distance between 2 solutions AFS_a and AFS_b is less than visual scope, AFS_b is the fish in the $N(AFS_a)$, where $N(AFS_a)$ is the neighbouring set of AFS_a. To keep the diversity of each solution as much as possible, the distance between 2 solutions is defined by the Equation (41) (Luo *et al.* 2015):

$$Dis(AFS_a, AFS_b) = \frac{\sum_{r=1}^{R}\left(c_k \left| sc_{a,r} = sc_{b,r'}, r' \in \{1,\ldots,R\}, c_k \in sc_{b,r'}\right.\right)}{N_C}, \quad (41)$$

where: N_C is the amount of customers in solution; R is the maximum amount of routes of the system; c_k is the customer in a route; $sc_{a,r}$ is the list of visits of the customers in the route r of AFS_a.

The preying behaviour is a kind of operator that AFS_a learns from the better state AFS_b in the $N(AFS_a)$ through a certain number *try_N* of random searches. The execute rule of the preying behaviour is described in the following. 1st, identify the same depot in AFS_b and AFS_a, then exchange the routes, which serviced by the depot, and delete the duplicate customers in the AFS_a. In this case, the number of customers may be missing in the AFS_a. 2nd, the missing customers are reinsert into AFS_a according to the minimum insertion cost calculated by Equation (42) to generate a new artificial fish AFS_{off}. In Equation (42), not only the extra distance and extra time is considered when customer c insert in the location u of the route r, the capacity constraint and the range constraint of the EV are also considered. Moreover, if the best feasible insertion place cannot be found, a new route will be opened and assigned to its nearest depot.

$$\begin{aligned} AIC_c = {} & \eta \cdot \big(\alpha_1 \cdot C_{11}(i,u,j) + \\ & \alpha_2 \cdot C_{12}(i,u,j) + \alpha_3 \cdot C_{13}(i,u,j)\big) + \\ & (1-\eta) \cdot \left(\sum_{w' \in W_r'} s_{w'} - \sum_{w \in W_r} s_w\right) + \\ & \Psi \cdot \max\left(\left(\sum_{c \in C_r} C_{ck}^{ev} - C^{ev}\right), 0\right), \end{aligned} \quad (42)$$

where: $\eta \in [0,1]$; s_w is the battery effectiveness of node w of route r, i.e., if $E_{wk}^{a} < 0$; $s_w = \left|E_{wk}^{a}\right|$, otherwise $s_w = 0$; W_r, W_r' are the node sets of route r before and after insertion, respectively; C_r is the customer set of route r after insertion.

The following behaviour is to learn from the optimal solution AFS_{best} in the $N(AFS_a)$. The swarming behaviour is to learn from the centre state in the $N(AFS_a)$ which is defined with the largest route repetition coefficient $LRRC$ in Equation (43). Both behaviours will be executed if their learning objects have higher food consistence and is not too crowded. The execute rules of 2 behaviours are the same as the execute rule of preying behaviour.

$$LRRC = \max_{b \in N(AFS_a)}\left(\sum_{r'=1}^{R}\sum_{c=1}^{|N(AF_a)|-1}(a)\right), \quad (43)$$

where: $a = \lambda \left| sc_{b,r'} = sc_{c,r''}, \ r'' \in \{1,\ldots,R\}, \lambda \in (0,1) \right.$; λ is binary decision variable indicating whether $sc_{b,r'} = sc_{c,r''}$.

If the preying, swarming and following behaviours cannot be executed, the random behaviour will be executed. The random behaviour is implemented for the AFS_a by 3 types of mutation operators (i.e., random customer selecting operator, random depot selecting operator and random charging-station selecting operator). The mutation operators are selected based on the weights, which are automatically adjusted according to their historical performances (Ropke, Pisinger 2006):

- *random* customer *selecting operator*. Select N_r customers at random and remove them from the AFS_a. Then place them back to the AFS_a based on the insertion cost calculated by Equation (42).

$$N_r = \left(\mu_1 + \left(\mu_2 - \mu_1\right) \cdot \mu_3\right) \cdot N_C, \tag{44}$$

where: μ_1, μ_2, μ_3 are the random number, $\mu_1, \mu_2 \in \left(0, 1\right)$, $\mu_1 \le \mu_2$, $\mu_3 \in \left[0, 1\right]$;

- *random depot selecting operator*. This operator is executed by randomly selecting Method 1 and Method 2. Method 1 indicates that randomly select one opened depot *d* and close it, then delete the customers, which served by *d*. Method 2 indicates that randomly select one opened depot *d* and close it, then delete the customers, which served by *d*, after that, select an unused depot by a roulette wheel mechanism. The probability of choosing an unused depot is inversely proportional to the distance from the *d*. In above 2 methods, the deleted customers are placed back to the solution based on Equation (42);
- *random charging-station selecting operator*. Remove routes with the maximum contribution CR_r defined by Equation (45) until N_r customers are removed, means removing routes that visit more charging-stations and fewer customers. The selected N_r customers are reinsert to the solution based on Equation (42).

$$CR_r = \frac{N_C^r + \tau \cdot N_S^r}{N_C^r + N_S^r}, \tag{45}$$

where: N_C^r, N_S^r are the amount of customers and charging-stations in route *r*, respectively; τ is a predefined parameter.

3.3. Charging-station optimization

Select a solution from the population in turn to optimize its location and size of charging-stations for each route by the proposed LCOA; then get a route set *R* from this solution; create an empty route set R^*:

- *Step 1*: select a route $r \in R$ and remove all of the charging-stations in route *r* and fix the order of customers. Create the current best route $r^* \leftarrow r$, and a route *TreeSet TS* and put *r* into *TS*. $\left|R\right| = \left|R\right| - 1$;
- *Step 2*: select and delete a route *r'* from *TS*. Calculate the remaining battery power B_w for each vertex in route *r'*. Let $B_{\min} = \min\{B_w\}_{\min}$. If $B_{\min} < 0$, find the 1st unreachable node w^* in route *r'*. Then identify suitable insertion points of the charging-stations in *CIL* with the minimum insertion costs, where *CIL* denotes the candidate insertion point set before w^*. Let $r'' \leftarrow r'$, and put *r''* into *TS*. If $B_{\min} \ge 0$, a comparison mechanism according to the label $\left(fs', tc', ns', vb', fl'\right)$ is adopted to select the best candidate route for the next extension, where *fs'* equals to 1 if the route is feasible, and 0 otherwise, *tc'* is the traveling cost, *ns'* is the amount of charging-stations in the route, *vb'* represents the amount of violated battery level, *fl'* represents the location of the 1st unreachable node (Jie *et al.* 2019). If label $\left(fs', tc', ns', vb', fl'\right)$ is better than label $\left(fs^*, tc^*, ns^*, vb^*, fl^*\right)$, let $r^* \leftarrow r$;
- *Step 3*: if *TS* is not empty, go to Step 2. Otherwise, put r^* into R^*;
- *Step 4*: if $\left|R\right| \ne 0$, go to Step 1. Otherwise, output a new route set R^*.

4. Computational experiments

4.1. Implementation and parameter configurations

As there are no available benchmark instances to assess the approaches for the ECC-LRP-CS, the instances with different number of customers are constructed. The number of customers is set to $\left|C\right| = \left\{20, 30, 40, 50, 60\right\}$, and the number of depots is to 5. All customers and depots are randomly located in the square interval $\left[0, 100\right]^2$ km in a uniform distribution. Each customer demand is randomly selected using a uniform distribution in the range $\left[10, 500\right]$ kg. The service time of each customer *i* is dependent on its total delivery demand, i.e., $t_i^s = 1800 \cdot \frac{d_i^c}{\sum_{i \in C} \frac{d_i^c}{C}}$ (Leng *et al.* 2020). The soft time windows of each customer are randomly selected using the method developed by Solomon (1987). Moreover, each depot capacity is randomly selected using a uniform distribution in the range $\left[3000, 7000\right]$ kg. The construction cost of each depot is also randomly generated using a uniform distribution in the range $\left[85000, 100000\right]$ ¥ (Koç *et al.* 2016). As the lifetime of each depot is set to 10 years, the construction cost of each depot can be converted into one day.

The number of charging-stations is set to $\left|S\right| = \left\{5, 7, 9, 11, 13\right\}$ and also randomly located in the square interval $\left[0, 100\right]^2$ km in a uniform distribution (Schneider *et al.* 2014). The construction cost of a candidate charging-station equals to 55.26 ¥, which is calculated by dividing their costs by the number of days within their lifetime (Çalık *et al.* 2021). Moreover, the battery driving range is set to 1.6 times the maximum Euclidean distance between any 2 nodes in the study area (Schneider *et al.* 2014). The capacity of the EVs is 1.33 tons. The utilization efficiency of the battery capacity is 90%. The minimal remaining battery power equals 10% of battery capacity. The renting cost of each EV, the driver salary and the fixed use cost for each EV are 15 ¥/h, 25 ¥/h and 70 ¥, respectively (Leng *et al.* 2020). The speed-related unit distance power consumption is calculated by $p_v^c = 324.69 \cdot v^{-0.228}$ (Zhou *et al.* 2016). The electricity price is 0.60 ¥/kW·h. The values of the parameters involving the traveling speed of the EV, the refrigeration cost in transportation and unloading process, the rate of deterioration in transportation and unloading process, the unit price of goods, the waiting and the late costs of unit time are given by Zhang *et al.* (2019c). Moreover, the parameters of visual scope, try number, crowd level are given by Song *et al.* (2020).

4.2. Computational results

In Figure 3, the Pareto front of 5 instances are presented. As expected, when the total penalty cost decreases, the cold chain logistics cost increases. This indicates that the conflict of the 2 objectives in model. In addition, to evaluate the performance of the integrated algorithm, this subsection firstly compares the results obtained by NA and the developed integrated algorithm, and then uses performance metrics to compare the RPF and the APF.

Li *et al.* (2017) state that the evaluation of algorithm contains the proximity to the RPF and the diversity among non-dominated solutions. In this study, generational distance I_{GD} (Zitzler *et al.* 2003), inverted generational distance I_{GD} (Zhou *et al.* 2017) are selected to measure the convergence and diversity of the obtained solutions, which are shown in Equations (46) and (47), respectively. Spacing I_S (Li *et al.* 2017) is the performance metric to measure the range variance of neighbouring solutions in the Pareto optimal solutions as defined in Equations (48) and (49).

$$I_{GD} = \frac{\sum_{i \in |APF|} Ed\left(APF\left(i\right), RPF\right)}{|APF|}; \tag{46}$$

$$I_{IGD} = \frac{\sum_{i \in |RPF|} Ed\left(RPF\left(i\right), APF\right)}{|RPF|}; \tag{47}$$

$$I_S = \sqrt{\frac{\sum_{i \in |RPF|}\left(\sum_{i \in |RPF|} \frac{d_{\min,i}}{|RPF|} - d_{\min,i}\right)^2}{|RPF| - 1}}; \tag{48}$$

$$d_{\min,i} = \min_{j \in |APF|}\left(\left|Z_1\left(RPF\left(i\right)\right) - Z_1\left(APF\left(j\right)\right)\right| + \left|Z_2\left(RPF\left(i\right)\right) - Z_2\left(APF\left(j\right)\right)\right|\right), \tag{49}$$

where: $Ed\left(APF\left(i\right), RPF\right)$ is the Euclidean distance between ith solution in the APF and its nearest point in the RPF; $Ed\left(RPF\left(i\right), APF\right)$ is the Euclidean distance between ith solution in the RPF and its nearest point in the APF; $|APF|$, $|RPF|$ are the cardinalities of APF and RPF, respectively; $d_{\min,i}$ is the minimal distance between 2 solutions.

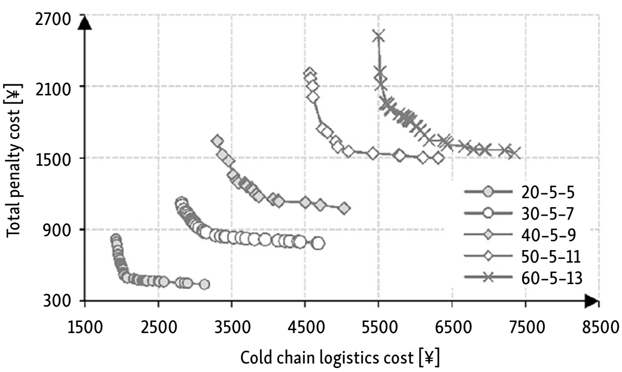

Figure 3. Pareto front of 5 instances

This study runs the integrated algorithm 20 times and records the best performance metrics. The RPF shows the results that are found in longer computing time, which equal to 2200. As shown in Table 1, $I_{1,GD}$, $I_{1,IGD}$ and $I_{1,S}$ are calculated by the results of the integrated algorithm with stopping conditions of 1000 iterations and 2200 iterations. $I_{2,GD}$, $I_{2,IGD}$ and $I_{2,S}$ are calculated by the results of the integrated algorithm with stopping conditions of 2000 iterations and 2200 iterations. It is clear that in each instance, the values of $I_{1,GD}$, $I_{2,GD}$, $I_{1,IGD}$ and $I_{2,IGD}$ are less than 0.05, which indicates that the better the distribution of the APF and the convergence of the developed algorithm is. Moreover, I_{GD} and I_{IGD} equal to 0 means that the APF is a part of the RPF and the APF is equal to the RPF, respectively. The values of $I_{1,S}$ and $I_{2,S}$ are less than 1, which indicates a uniform distribution of solutions in the APF. In addition, I_S equal to 0 reveals that the APF is equidistantly placed.

Table 1. Results of the performance metrics

Instance	$I_{1,GD}$	$I_{2,GD}$	$I_{1,IGD}$	$I_{2,IGD}$	$I_{1,S}$	$I_{2,S}$
20–5–5	0.000	0	0.008	0.000	0.055	0.000
30–5–7	0.000	0	0.023	0.000	0.245	0.000
40–5–9	0.002	0	0.016	0.001	0.301	0.001
50–5–11	0.001	0	0.025	0.000	0.619	0.001
60–5–13	0.002	0	0.040	0.001	0.890	0.002

4.3. Comparison between NA and heuristic

Although the NA is relatively accurate, the computational workload is heavier. The iteration of the heuristic is nondeterministic, but the computational efficiency is ideal. In view of this difference, this section compares the performance of these 2 algorithms under the different driving principles of "accuracy" and "efficiency".

The NA based on a model linearization and a parallel branch & bound is used to solve the ECC-LRP-CS. Firstly, transform the 2 objectives into a single one. As this model is in the form of 0–1 programming, the method of "element filling" introduced by Verma *et al.* (2012) is used to make the 2 objectives consistent in magnitude. Let $\mathbf{X} = \left(X_{ijk}, Y_j, Z_s\right)^T$, then $\mathbf{X}_1^{only} = \left(1, \ldots, 1\right)^T$, $\mathbf{X}_0^{only} = \left(0, \ldots, 0\right)^T$. So $Z_1' = \frac{Z_1}{\left|Z_1\left(\mathbf{X}_1^{only}\right) - Z_1\left(\mathbf{X}_0^{only}\right)\right|}$, $Z_2' = \frac{Z_2}{\left|Z_2\left(\mathbf{X}_1^{only}\right) - Z_2\left(\mathbf{X}_0^{only}\right)\right|}$.

If $Z_1\left(\mathbf{X}_1^{only}\right) - Z_1\left(\mathbf{X}_0^{only}\right) = 0$ or $Z_2\left(\mathbf{X}_1^{only}\right) - Z_2\left(\mathbf{X}_0^{only}\right) = 0$, replace $\mathbf{X}_1^{only}$ with $\mathbf{X}_{0.5}^{only}$. If the condition of "non-zero" still doesn't hold, replace $\mathbf{X}_1^{only}$ with $\mathbf{X}_{(0.5)^2}^{only}$, and so on by $\mathbf{X}_{(0.5)^n}^{only}$. After that, the weighting coefficient $\lambda \in \left(0, 1\right)$ is introduced to transform the objective function as shown in Equation (50). The constraints in MD_1 model are the same in multi-objective optimization model.

$$MD_1 \quad Z = \min\left(\lambda \times Z_1 + \left(1 - \lambda\right) \times Z_2\right) \tag{50}$$

subject to: Equations (12)–(36).

Next, in order to facilitate the derivation and description, the MD_1 model is simply represented as MD_2, i.e., let $\min\left(\lambda \times Z_1' + (1-\lambda) \times Z_2'\right) = \min_{\chi}\left(\boldsymbol{\chi}^{T_1^{T_{23}}}\right)$, as shown in (51)–(53). For MD_2, the dimension of solution space is $\eta = \eta_1 + \eta_2 + \eta_3 + \eta_1 \cdot \eta_3 + \eta_2 \cdot \eta_3 + \eta_1 \cdot \eta_2 + \eta_3 \cdot \eta_3$. η_1 and η_2 are the numbers of candidates for depots/charging-stations, respectively. η_3 is the numbers of customers. $\boldsymbol{A}_1$ is the matrix of coefficients of quadratic terms in the objective. All elements in $\boldsymbol{A}_1$ are non-negative, and the order of $\boldsymbol{A}_1$ is $\eta \times \eta$. $\boldsymbol{A}_2$ is the matrix of coefficients of linear terms in the objective. The order of $\boldsymbol{A}_2$ is $\eta \times 1$. $\boldsymbol{A}_3$ is the matrix of constants in the objective. $\boldsymbol{B}$ is the matrix of coefficients corresponding to the constraints. The order of $\boldsymbol{B}$ is $\sigma \times \eta$, where σ is the number of constraints of MD_1. In addition, $\boldsymbol{b}$ is a constant matrix with the order of $\sigma \times 1$.

$$MD_2 \ \min_{\chi} f(\boldsymbol{\chi}) = \min_{\chi}\left(\boldsymbol{\chi}^{T_1^{T_{23}}}\right) \tag{51}$$

subject to:

$$\mathrm{B} \cdot \boldsymbol{\chi} \geq \mathrm{b}; \tag{52}$$

$$\boldsymbol{\chi} \in \{0, 1\}^{\eta}. \tag{53}$$

After that, with the vector $\mathrm{e} = (1, ..., 1)^T$, an equivalent linear model MD_3 can be obtained, as shown in Equations (54)–(60):

$$MD_3 \ \min_{\mu, \chi, y} f(\boldsymbol{\mu}, \boldsymbol{\chi}) = \min_{\chi}\left(\mathrm{e}^{T^{T_{23}}}\right) \tag{54}$$

subject to:

$$\mathrm{A}_1 \cdot \boldsymbol{\chi} - \mathrm{y} - \boldsymbol{\mu} = 0; \tag{55}$$

$$\mathrm{B} \cdot \boldsymbol{\chi} \geq \mathrm{b}; \tag{56}$$

$$\mathrm{y} \leq M(\mathrm{e} - \boldsymbol{\chi}); \tag{57}$$

$$\boldsymbol{\chi} \in \{0, 1\}^{\eta}; \tag{58}$$

$$\mathrm{y} = \left(y_1, ..., y_h, ..., y^{\eta}\right)^T, \ y_h \geq 0; \tag{59}$$

$$\boldsymbol{\mu} = \left(\mu_1, ..., \mu_h, ..., \mu^{\eta}\right)^T, \ \mu_h \geq 0. \tag{60}$$

Finally, for the linear model MD_3, it contains more auxiliary variables and additional constraints. Therefore, a parallel branch and bound process is designed in this study to achieve high computational efficiency. This process is started by initialling solution with $\boldsymbol{\chi}_{Ini} = (0, ..., 0)^T$. Then the sequence of the solution is updated similar to the arithmetic sequence of binary numbers. After that, judge the objective and check the current solution with constraints. If any element in the termination solution meets $\boldsymbol{\chi}_h = 1$, that is, $\boldsymbol{\chi}_{End} = (1, ..., 1)^T$, the update of solution is terminated and output the current feasible solution $\boldsymbol{\chi}_{Fea}$ and the corresponding objective Z^*.

This study solves the instances with the integrated algorithm and compares the intermediate solution of the obtained Pareto front to the optimal solution found by the linear model MD_3 (Jabbarzadeh *et al.* 2020). As shown in Table 2, t_{OT} represents operation time. With increasing problem scale, the calculating time of the NA increases much more significantly. In comparison with the NA, the developed integrated algorithm has outstanding advantages in operation time. That is, the developed integrated algorithm has a high efficiency for tackling the model under different data sizes, and is able to achieve good results at appropriate calculating time. Moreover, the deviation value between results obtained with the NA and the developed integrated algorithm increases with increasing problem scale, which reveals that longer calculating time and more iterations are required for better solutions. For the larger problem scale with 60 customers, the deviation values are acceptable at certain calculating time. Therefore, when the problem scale is large, the developed integrated algorithm can be used as a reasonable and feasible approach. Furthermore, as the cold chain logistics demand increases, both the cold chain logistics cost and the total penalty cost increase.

4.4. Sensitivity analysis

The integrated algorithm is performed 20 times to empirically assess the effects of battery driving range and traveling speed by using the small instance with 20 customers and the larger instance with 60 customers. The intermediate solutions of the obtained Pareto front are selected as the objectives.

In the experiments, this study decreases the battery driving range by 10%, 20%, 30% and 40%, and increases it by 10%, 20%, 30% and 40%, respectively. As shown in Figure 4 and Figure 5, both the cold chain logistics cost and the total penalty cost decrease as the battery driving range of EVs increases. The reason for this is that as the battery driving range is increased, the detours of EVs decrease, thus decreasing the traveling time of EVs. As a result, the renting cost of EVs, the driver salary, power consumption cost during the transportation, refrigeration cost during

Table 2. Performance comparison between 2 algorithms

Instance	NA					Integrated Algorithm		
	Z	Z_1	Z_2	λ^*	t_{OT}	Z_1	Z_2	t_{OT}
20–5–5	967.19	2059.35	499.12	0.3	4 min 47 s	2065.17	500.56	4 min 72 s
30–5–7	1554.00	3142.98	873.01	0.3	7 min 0 s	3154.79	876.19	5 min 86 s
40–5–9	1998.23	3760.12	1243.14	0.3	14 min 42 s	3775.96	1248.31	10 min 9 s
50–5–11	3071.41	4917.85	1577.53	0.4	28 min 5 s	4942.25	1592.24	11 min 27 s
60–5–13	3593.59	5848.44	1791.73	0.4	51 min 5 s	5902.78	1821.05	13 min 53 s

transportation and the damage cost for the transportation process are reduced. Moreover, as the traveling time of EVs decreases, the charging times of EVs decrease, thus reducing the recharging cost. In addition, because of the detours of EVs decreasing, the punctuality rate of arriving at customers will improve, thus reducing the time penalty cost. Furthermore, the reduction of battery driving range may lead to open new delivery routes, then the number of EVs increases, thus increasing the fixed use cost for EVs. At the same time, it may lead to open new depots. However, the number of charging-stations reveals little variation as battery driving range increases. The reason is that a charging-station can service a same EV more than once. Therefore, if the charging-stations locate in a suitable location, the amount of charging-stations will be decreased, but not much. Therefore, to save the cost of the cold chain logistic network, the EVs with larger battery driving range need to give a priority to use to deliver goods by logistics enterprises. At the same time, the selection of the type of EVs requires balancing the renting cost of EVs and the battery driving range according to the real service scope and volume of the logistics enterprises.

The influences of traveling speed of EVs on the results are analysed. The traveling speed (by –10%, –20%, –30%, –40%, 10%, 20%, 30% and 40%) on each arc is changed. As shown in Figure 6 and Figure 7, as the traveling speed increases, the traveling time reduces, thus decreasing the cost of renting EVs, the driver salary, the power consumption cost, the refrigeration cost during transportation, the damage cost for the traveling process and the time penalty cost. As a result, the cold chain logistics cost and the total penalty cost decrease. However, if the traveling speed increases too much, both the cold chain logistics cost and the total penalty cost increase. The reason for this is that the power consumption cost favours a suitable traveling speed. In addition, if the traveling speed is too high, the EVs will arrive earlier at customers, thus increasing the waiting time penalty of EVs.

5. Conclusions

With the development of the EV technology, the EV cold chain logistics network optimization problem has become a current focus for research to control the carbon emission. Therefore, an ECC-LRP-CS is proposed in this study to achieve sustainable development targets including reducing carbon emission and logistics cost, and improving customer satisfaction. A multi-objective optimization model is established to tackle this problem. The 1st objective consists of 6 components, i.e., fixed cost, variable cost, power consumption cost, refrigeration cost, recharging cost and construction cost for charging-stations. The time penalty cost and the cargo damage cost are considered as the 2nd objective. Several practical constraints, such as soft time windows, capacity limitation of depot, energy consumption of EVs, are considered in the developed model. An integrated algorithm that combines an IAFSA and a LCOA is applied for the proposed framework.

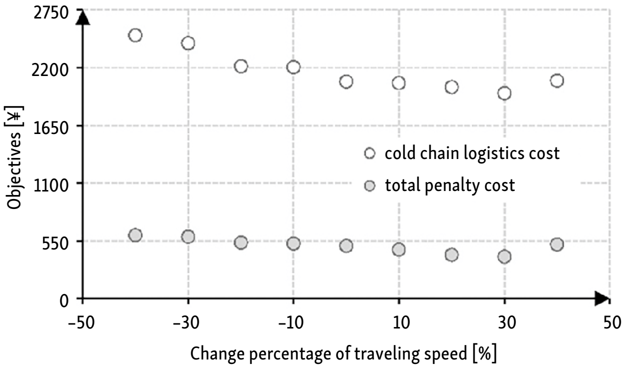

Figure 4. Effects of battery driving range on the small instance

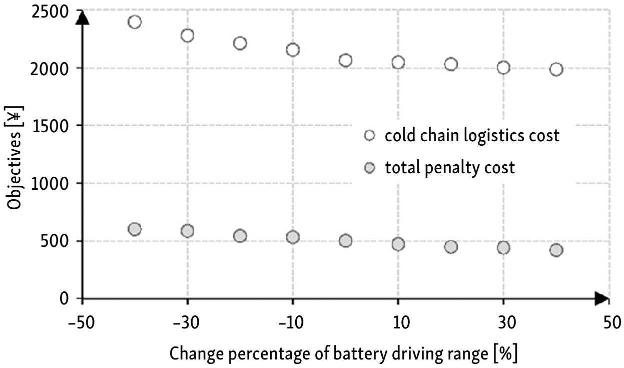

Figure 5. Effects of battery driving range on the larger instance

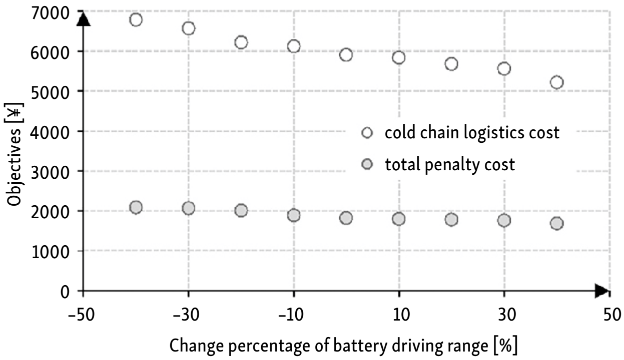

Figure 6. Effects of traveling speed on the small instance

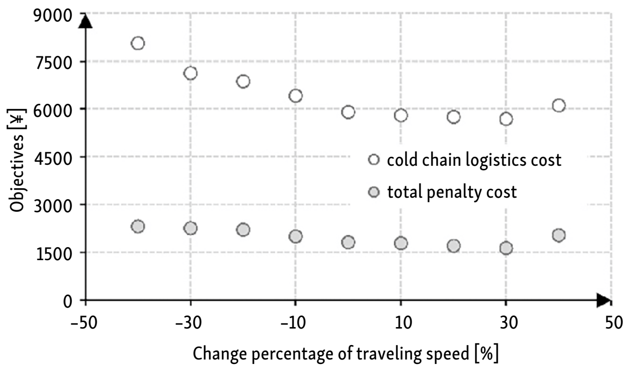

Figure 7. Effects of traveling speed on the larger instance

Moreover, to evaluate the performance of the developed approach, the comparison with NA and the performance metrics are used. Extensive experiments are conducted to measure the effects of battery driving range and traveling speed on the Pareto front.

This study still has several limitations:

- 1st, case studies on large and realistic cold chain logistics networks are necessary to further access the performance of the presented model and algorithm;
- 2nd, the dynamic designs of delivery services should be made in consideration of real traffic conditions, changeable customer demand, types of cargos, charging-station capacity, etc. in future work;
- 3rd, the developed integrated algorithm needs to have more values of different parameters and variables tested and compare with other known algorithms applied to the similar problems to further validate and improve its application effectiveness and efficiency in future research. Finally, to control the carbon emission, the government policies such as subsidy policy (Zhang *et al.* 2019a), carbon tax (Wang *et al.* 2017; Zhang *et al.* 2018) and carbon emissions trading policy (Liu *et al.* 2020a) should be researched to guide cold chain logistics enterprises in a way of reasonable and effective emission reduction.

Funding

This work was supported by the Youth Foundation of Beijing Wuzi University (China) (Grant No 2022XJQN08).

Disclosure statement

It is declared that there is no conflict of interests regarding the publication of this article.

Declaration on the use of Artificial Intelligence (AI)

During the preparation of this article, the author did not use generative AI or AI-assisted technologies and takes full responsibility for the content of this article.

References

Azad, M. A. K.; Rocha, A. M. A. C.; Fernandes, E. M. G. P. 2014. Improved binary artificial fish swarm algorithm for the 0–1 multidimensional knapsack problems, *Swarm and Evolutionary Computation* 14: 66–75. https://doi.org/10.1016/j.swevo.2013.09.002

Bac, U.; Erdem, M. 2021. Optimization of electric vehicle recharge schedule and routing problem with time windows and partial recharge: a comparative study for an urban logistics fleet, *Sustainable Cities and Society* 70: 102883. https://doi.org/10.1016/j.scs.2021.102883

Çalık, H.; Oulamara, A.; Prodhon, C.; Salhi, S. 2021. The electric location-routing problem with heterogeneous fleet: formulation and Benders decomposition approach, *Computers & Operations Research* 131: 105251. https://doi.org/10.1016/j.cor.2021.105251

Eggers, Fe.; Eggers, Fa. 2011. Where have all the flowers gone? Forecasting green trends in the automobile industry with a choice-based conjoint adoption model, *Technological Forecasting and Social Change* 78(1): 51–62. https://doi.org/10.1016/j.techfore.2010.06.014

Ghobadi, A.; Tavakkoli Moghaddam, R.; Fallah, M. 2021. Multi-depot electric vehicle routing problem with fuzzy time windows and pickup/delivery constraints, *Journal of Applied Research on Industrial Engineering* 8(1): 1–18.

He, Q.; Hu, X.; Ren, H.; Zhang, H. 2015. A novel artificial fish swarm algorithm for solving large-scale reliability–redundancy application problem, *ISA Transactions* 59: 105–113. https://doi.org/10.1016/j.isatra.2015.09.015

Hof, J.; Schneider, M.; Goeke, D. 2017. Solving the battery swap station location-routing problem with capacitated electric vehicles using an AVNS algorithm for vehicle-routing problems with intermediate stops, *Transportation Research Part B: Methodological* 97: 102–112. https://doi.org/10.1016/j.trb.2016.11.009

Jabbarzadeh, A.; Azad, N.; Verma, M. 2020. An optimization approach to planning rail hazmat shipments in the presence of random disruptions, *Omega* 96: 102078. https://doi.org/10.1016/j.omega.2019.06.004

James, S. J.; James, C. 2010. The food cold-chain and climate change, *Food Research International* 43(7): 1944–1956. https://doi.org/10.1016/j.foodres.2010.02.001

Jie, W.; Yang, J.; Zhang, M.; Huang, Y. 2019. The two-echelon capacitated electric vehicle routing problem with battery swapping stations: formulation and efficient methodology, *European Journal of Operational Research* 272(3): 879–904. https://doi.org/10.1016/j.ejor.2018.07.002

Jung, J.; Jayakrishnan, R. 2012. High-coverage point-to-point transit: electric vehicle operations, *Transportation Research Record: Journal of the Transportation Research Board* 2287: 44–53. https://doi.org/10.3141/2287-06

Koç, Ç.; Bektaş, T.; Jabali, O.; Laporte, G. 2016. The fleet size and mix location-routing problem with time windows: formulations and a heuristic algorithm, *European Journal of Operational Research* 248(1): 33–51. https://doi.org/10.1016/j.ejor.2015.06.082

Leng, L.; Zhang, C.; Zhao, Y.; Wang, W.; Zhang, J.; Li, G. 2020. Biobjective low-carbon location-routing problem for cold chain logistics: Formulation and heuristic approaches, *Journal of Cleaner Production* 273: 122801. https://doi.org/10.1016/j.jclepro.2020.122801

Li, L.; Wang, W.; Xu, X. 2017. Multi-objective particle swarm optimization based on global margin ranking, *Information Sciences 375*: 30–47. https://doi.org/10.1016/j.ins.2016.08.043

Li, X.; Shao, Z. 2002. An optimizing method based on autonomous animals: fish-swarm algorithm, *Systems Engineering – Theory & Practice* 22(11): 32–38. https://doi.org/10.3321/j.issn:1000-6788.2002.11.007 (in Chinese).

Lin, C. K. Y.; Kwok, R. C. W. 2006. Multi-objective metaheuristics for a location-routing problem with multiple use of vehicles on real data and simulated data, *European Journal of Operational Research* 175(3): 1833–1849. https://doi.org/10.1016/j.ejor.2004.10.032

Liu, G.; Hu, J.; Yang, Y.; Xia, S.; Lim, M. K. 2020a. Vehicle routing problem in cold chain logistics: a joint distribution model with carbon trading mechanisms, *Resources, Conservation and Recycling* 156: 104715. https://doi.org/10.1016/j.resconrec.2020.104715

Liu, Y.; Feng, X., Zhang, L.; Hua, W.; Li, K. 2020b. A Pareto artificial fish swarm algorithm for solving a multi-objective electric

transit network design problem, *Transportmetrica A*: *Transport Science* 16(3): 1648–1670.
https://doi.org/10.1080/23249935.2020.1773574

Luo, J.; Li, X.; Chen, M.-R.; Liu, H. 2015. A novel hybrid shuffled frog leaping algorithm for vehicle routing problem with time windows, *Information Sciences* 316: 266–292.
https://doi.org/10.1016/j.ins.2015.04.001

Ropke, S.; Pisinger, D. 2006. An adaptive large neighborhood search heuristic for the pickup and delivery problem with time windows, *Transportation Science* 40(4): 455–472.
https://doi.org/10.1287/trsc.1050.0135

Sassi, O.; Oulamara, A. 2017. Electric vehicle scheduling and optimal charging problem: complexity, exact and heuristic approaches, *International Journal of Production Research* 55(2): 519–535. https://doi.org/10.1080/00207543.2016.1192695

Sayarshad, H. R.; Mahmoodian, V.; Gao, H. O. 2020. Non-myopic dynamic routing of electric taxis with battery swapping stations, *Sustainable Cities and Society* 57: 102113.
https://doi.org/10.1016/j.scs.2020.102113

Schiffer, M.; Walther, G. 2017. The electric location routing problem with time windows and partial recharging, *European Journal of Operational Research* 260(3): 995–1013.
https://doi.org/10.1016/j.ejor.2017.01.011

Schneider, M.; Stenger, A.; Goeke, D. 2014. The electric vehicle-routing problem with time windows and recharging stations, *Transportation Science* 48(4): 500–520.
https://doi.org/10.1287/trsc.2013.0490

Solomon, M. M. 1987. Algorithms for the vehicle routing and scheduling problems with time window constraints, *Operations Research* 35(2): 254–265. https://doi.org/10.1287/opre.35.2.254

Song, M.-X.; Li, J.-Q.; Han, Y.-Q.; Han, Y.-Y.; Liu, L.-L., Sun, Q. 2020. Metaheuristics for solving the vehicle routing problem with the time windows and energy consumption in cold chain logistics, *Applied Soft Computing* 95: 106561.
https://doi.org/10.1016/j.asoc.2020.106561

Verma, M.; Verter, V.; Zufferey, N. 2012. A bi-objective model for planning and managing rail-truck intermodal transportation of hazardous materials, *Transportation Research Part E*: *Logistics and Transportation Review* 48(1): 132–149.
https://doi.org/10.1016/j.tre.2011.06.001

Wang, S.; Tao, F.; Shi, Y.; Wen, H. 2017. Optimization of vehicle routing problem with time windows for cold chain logistics based on carbon tax, *Sustainability* 9(5): 694.
https://doi.org/10.3390/su9050694

Yang, J.; Sun, H. 2015. Battery swap station location-routing problem with capacitated electric vehicles, *Computers* & *Operations Research* 55: 217–232. https://doi.org/10.1016/j.cor.2014.07.003

Yang, W.-H. 2014. An improved artificial fish swarm algorithm and its application in multiple sequence alignment, *Journal of Computational and Theoretical Nanoscience* 11(3): 888–892.

Yu, V. F.; Normasari, N. M. E.; Chen, W.-H. 2021. Location-routing problem with time-dependent demands, *Computers* & *Industrial Engineering* 151: 106936.
https://doi.org/10.1016/j.cie.2020.106936

Zhang, D. Z.; Eglese, R.; Li, S. 2018. Optimal location and size of logistics parks in a regional logistics network with economies of scale and CO_2 emission taxes, *Transport* 33(1): 52–68.
https://doi.org/10.3846/16484142.2015.1004644

Zhang, S.; Chen, N.; Song, X.; Yang, J. 2019a. Optimizing decision-making of regional cold chain logistics system in view of low-carbon economy, *Transportation Research Part A*: *Policy and Practice* 130: 844–857. https://doi.org/10.1016/j.tra.2019.10.004

Zhang, S.; Chen, M.; Zhang, W. 2019b. A novel location-routing problem in electric vehicle transportation with stochastic demands, *Journal of Cleaner Production* 221: 567–581.
https://doi.org/10.1016/j.jclepro.2019.02.167

Zhang, L.-Y.; Tseng, M.-L.; Wang, C.-H.; Xiao, C.; Fei, T. 2019c. Low-carbon cold chain logistics using ribonucleic acid-ant colony optimization algorithm, *Journal of Cleaner Production* 233: 169–180. https://doi.org/10.1016/j.jclepro.2019.05.306

Zhang, S.; Chen, M.; Zhang, W.; Zhuang, X. 2020. Fuzzy optimization model for electric vehicle routing problem with time windows and recharging stations, *Expert Systems with Applications* 145: 113123. https://doi.org/10.1016/j.eswa.2019.113123

Zhang, Z.; Wang, K.; Zhu, L.; Wang, Y. 2017. A Pareto improved artificial fish swarm algorithm for solving a multi-objective fuzzy disassembly line balancing problem, *Expert Systems with Applications* 86: 165–176.
https://doi.org/10.1016/j.eswa.2017.05.053

Zhao, Z.; Li, X.; Zhou, X. 2020. Distribution route optimization for electric vehicles in urban cold chain logistics for fresh products under time-varying traffic conditions, *Mathematical Problems in Engineering* 2020: 9864935.
https://doi.org/10.1155/2020/9864935

Zhou, Bo.; Wu, Y.; Zhou, Bi.; Wang, R.; Ke, W.; Zhang, S.; Hao, J. 2016. Real-world performance of battery electric buses and their life-cycle benefits with respect to energy consumption and carbon dioxide emissions, *Energy* 96: 603–613.
https://doi.org/10.1016/j.energy.2015.12.041

Zhou, Y.; Chen, Z.; Zhang, J. 2017. Ranking vectors by means of the dominance degree matrix, *IEEE Transactions on Evolutionary Computation* 21(1): 34–51.
https://doi.org/10.1109/tevc.2016.2567648

Zitzler, E.; Thiele, L., Laumanns, M.; Fonseca, C. M.; Da Fonseca, V. G. 2003. Performance assessment of multiobjective optimizers: an analysis and review, *IEEE Transactions on Evolutionary Computation* 7(2): 117–132.
https://doi.org/10.1109/tevc.2003.810758